Biol Cybern (2007) 96:341–350
DOI 10.1007/s00422-006-0120-6

ORIGINAL PAPER

Biological Cybernetics

A model of open-loop control of equilibrium position and stiffness of the human elbow joint

Dinant A. Kistemaker · Arthur J. (Knoek) Van Soest · Maarten F. Bobbert

Received: 15 November 2004 / Accepted: 14 October 2006 / Published online: 15 December 2006

Abstract According to the equilibrium point theory, the control of posture and movement involves the setting of equilibrium joint positions (EP) and the independent modulation of stiffness. One model of EP control, the α-model, posits that stable EPs and stiffness are set open-loop, i.e. without the aid of feedback. The purpose of the present study was to explore for the elbow joint the range over which stable EPs can be set open-loop and to investigate the effect of co-contraction on intrinsic low-frequency elbow joint stiffness (K_{ilf}). For this purpose, a model of the upper and lower arm was constructed, equipped with Hill-type muscles. At a constant neural input, the isometric force of the contractile element of the muscles depended on both the myofilamentary overlap and the effect of sarcomere length on the sensitivity of myofilaments to $[Ca^{2+}]$ (LDCS). The musculoskeletal model, for which the parameters were chosen carefully on the basis of physiological literature, captured the salient isometric properties of the muscles spanning the elbow joint. It was found that stable open-loop EPs could be achieved over the whole range of motion of the elbow joint and that K_{ilf}, which ranged from 18 to 42 N m·rad^{-1}, could be independently controlled. In the model, LDCS contributed substantially to K_{ilf} (up to 25 N m·rad^{-1}) and caused K_{ilf} to peak at a sub-maximal level of co-contraction.

List of Symbols

K_{ilf}	Intrinsic low-frequency joint stiffness
MEF	Mono-articular elbow flexor
BE	Bi-articular elbow extensor
STIM	Muscle stimulation
q	Active state
φ_e	Elbow angle
φ_e	Shoulder angle
CE	Contractile element
SE	Series elastic element
PE	Parallel elastic element
F_{CE}	Force delivered by CE
F_{MAX}	Maximum isometric force
F_{isom_n}	F_{CE}/F_{MAX}
l_{MTC}	Muscle-tendon complex length
l_{CE}	CE length
l_{CE_opt}	CE optimum length
l_{CE_rel}	l_{CE}/l_{CE_opt}
l_{PE}	PE length
l_{PE_0}	PE slack length
l_{SE}	SE length
l_{SE_0}	SE slack length

1 Introduction

Several theories have been proposed about how humans control movements. One of the most influential theories is the equilibrium point (EP) theory. The EP theory postulates that, because of the "spring-like" behavior of the (neuro-)musculoskeletal system, EPs are defined and that movements are made by shifting the EPs, with EPs being joint angles at which the net muscle moment equals zero. This theory is attractive from a computational point of view, because it does not rely on

D. A. Kistemaker (✉) · A. J (Knoek) Van Soest · M. F. Bobbert
Institute for Fundamental and Clinical Human Movement Sciences, IFKB, Vrije Universiteit, Van der Boechorststraat 9, 1081 BT Amsterdam, The Netherlands
e-mail: d.kistemaker@fbw.vu.nl

extensive computation to calculate the torque-time history required to move a system to a desired position. It is generally accepted that the spring-like behavior emerges from both intrinsic properties of muscles and reflexive pathways.

Intrinsic muscle properties are the essential component in a version of the EP hypothesis known as the α-model (e.g. Hogan 1984; Bizzi and Abend 1983). The central idea behind the α-model is that, due to the force–length properties of the muscles spanning a joint, a desired EP can be set by setting appropriate open-loop stimulation levels of these muscles. For this idea to work, it should be possible to specify open-loop stable EPs over the full range of motion of the joint to be controlled. In addition, it is desirable that at any EP, intrinsic stiffness, i.e. the stiffness provided by the muscles without neural feedback, can be adjusted to task requirements by means of co-contraction. Needless to say, these conditions are necessary but not sufficient for alpha-control to be feasible.

In animal experiments, the existence of stable EPs has indeed been confirmed. For example, it was shown by Giszter et al. (1993) that microstimulation of specific locations in the grey matter of the spinal cord of deafferented frogs elicited force fields that defined stable EPs of the frog's leg. It was suggested in that study that even though the number of force fields found was very small, equilibrium at any desired position would be achievable by combining these force fields. Similarly, Graziano et al. (2002) were able to set stable hand positions of monkeys by microstimulation of their primary motor and premotor cortex; constant stimulation of a specific part of the cortex led to movements that halted at a certain position, irrespective of the initial position of the limb. Again, there seemed to be a mapping from stimulation site at the cortex to equilibrium hand position in space. Tehovnik (1995) found similar results for orbital eye position with microstimulation in the dorsomedial frontal cortex of monkeys. However, because the system was neurophysiologically intact in the latter two studies, it was impossible to assess whether the observed equilibrium positions were due solely to the intrinsic muscle properties. Thus, while it has been shown in deafferented frogs that open-loop stimulation may define EPs, it is currently unclear to what extent this is also true in primates, and over what range of motion it holds.

Separation of intrinsic and reflexive contributions to the mechanical behavior of the controlled system is relevant from a control theoretical perspective, as both contributions have their advantages and disadvantages. The intrinsic contribution has the advantage of generating an immediate (zero-lag) response to perturbation, but prolonged modulation of the associated stiffness through co-contraction is energetically unattractive. This disadvantage does not apply to the reflexive contribution. However, time delays in the feedback loop set limits on the feedback gains at which the controlled system is stable, and thus on the reflexive contribution to the mechanical behavior of the controlled system.

Experimentally it is not trivial to determine the intrinsic and reflexive contributions to the total low-frequency joint stiffness (K_{ilf}), defined here as the change in steady-state muscle moment per unit change in steady-state joint angle, at constant muscle stimulation. For example, attempts to determine the (total) low-frequency joint stiffness using experiments in which subjects were asked to resist perturbations have resulted in values for elbow stiffness that range from $14\,\mathrm{N\,m{\cdot}rad^{-1}}$ (Bennet et al. 1992) to $126\,\mathrm{N\,m{\cdot}rad^{-1}}$ (Lacquaniti et al. 1982). Furthermore, separation of the reflexive and intrinsic contributions to the total low-frequency joint stiffness requires advanced system identification methods (e.g. Kearney et al. 1997; Van der Helm et al. 2002; it is currently unclear to what extent the results of these methods depend on the assumptions made.

From a modeling perspective, the existence of open-loop EPs and the contribution of intrinsic muscle properties to K_{ilf} at any joint depend on the static moment–angle–stimulation relationships of the muscles spanning that joint. As the parameters determining this relationship are well documented, we propose to take these as a starting point for a model-based exploration of open-loop control of EPs and K_{ilf}. To be more precise, the moment–angle–stimulation relation depends on the following relationships: the relationship between the force of the contractile element (F_{CE}), CE length (l_{CE}) and muscle stimulation (STIM), and the relationship between the length of muscle–tendon complexes (l_{MTC}) and joint angles. The latter relationship can be readily obtained in cadaver studies using the tendon displacement method (Grieve et al. 1978). The dependence of isometric F_{CE} on l_{CE} is commonly attributed to the overlap of actin and myosin combined with the effect of sarcomere length on the sensitivity of myofilaments to $[Ca^{2+}]$. This length-dependent $[Ca^{2+}]$ sensitivity (LDCS) causes the optimum muscle length to depend on stimulation (e.g. Roszek et al. 1994; Balnave and Allen 1996; Zuurbier et al. 1998; Hansen et al. 2003) and adds to the intrinsic low-frequency stiffness of a muscle (Kistemaker et al. 2005).

The purpose of the present study was to explore for a representative joint the range of motion over which stable EPs can be set open-loop and to investigate the effect of co-contraction on K_{ilf}. Because many experiments concerning stiffness involve the elbow joint, and because arm muscle parameters are well documented,

a model of the upper and lower arm was constructed. The model incorporated Hill-type muscle models and a formulation of LDCS (Hatze's 1981).

2 Methods

The model of the arm consisted of three rigid segments, interconnected by two hinges representing the glenohumeral and elbow joint, and was constrained to move in the horizontal plane (see Fig. 1). Segment parameter values were taken from Winter (1990; see Table 1). The muscles actuating the arm were lumped to end up with a mono-articular elbow flexor MEF (*brachioradialis, brachialis, pronator teres, extensor carpi radialis*), a mono-articular elbow extensor MEE (*triceps lateralis, triceps medialis, anconeus, extensor carpi ulnaris*), a bi-articular elbow flexor BF (*biceps long head, biceps short head*) and a bi-articular elbow extensor BE (*triceps long head*).

The modelled Hill-type muscles consisted of a contractile element (CE), a series elastic element (SE) and a parallel elastic element (PE), as shown schematically in Fig. 2. The relation between STIM and active state (q), the relative amount of Ca^{2+} bound to troponin (Ebashi and Endo 1968), was modelled following Hatze's (1981)

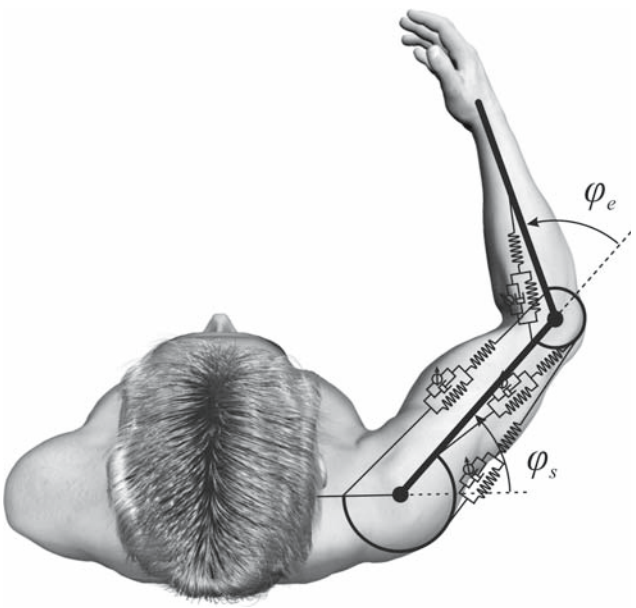

Fig. 1 Schematic drawing of the musculoskeletal model of the arm. The model consisted of three rigid segments interconnected by two hinges representing glenohumeral and elbow joint, actuated by four Hill-type muscles. φ_e = elbow angle and φ_s = shoulder angle. The model was constrained to move in the horizontal plane only

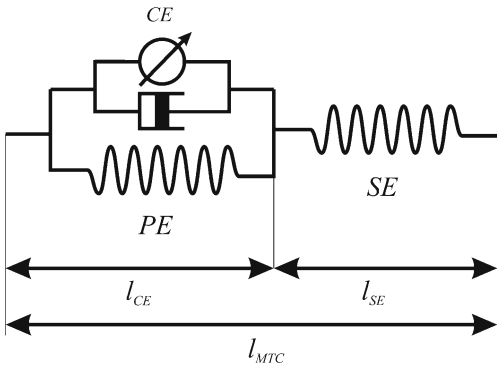

Fig. 2 Schematic representation of the Hill-type muscle model used in this study. See Appendix and "List of symbols" for abbreviations

and has been described in detail elsewhere (Kistemaker et al. 2005). SE and PE were modelled as quadratic springs. The isometric force delivered by CE depended on l_{CE} and q, and was described by a parabola determined by optimum l_{CE} (l_{CE_opt}), maximum isometric force (F_{MAX}), and a factor (*width*) specifying the zero crossings of the isometric force relative to l_{CE_opt}. A more detailed description of the muscle model is provided in the Appendix.

The muscle parameters, F_{MAX}, tendon slack-length (l_{SE_0}), l_{CE_opt} and moment arms of the four lumped muscles were obtained from Nijhof and Kouwenhoven (2000) and Murray et al. (1995, 2000). The contribution of the individual muscle parameters to the parameters of the lumped muscles depended on the relative contribution of the muscle to the total joint moment. Moment arms (arm) were related to joint angle on the basis of the relationship between the length of the muscle–tendon complex (l_{MTC}) and joint angle (Nijhof and Kouwenhoven 2000; Murray et al. 1995), measured using the tendon displacement method (Grieve et al. 1978). The muscle parameter *width* (see Appendix) was chosen such that the isometric elbow moment–angle relationship at maximal stimulation was in accordance with that observed experimentally (Singh and Karpovitch 1968; Kullig et al. 1984; Van Zuylen et al. 1988; An et al. 1989; Chang et al. 1999). Other non-specific muscle parameters were obtained from Van Soest and Bobbert (1993). All parameter values are presented in Tables 1 and 2.

To minimize the number of independent model inputs and to have a straightforward and meaningful definition of co-contraction, the stimulation levels of the mono- and bi-articular elbow extensors (STIMe) were set to be equal, and so were the stimulation levels of mono- and bi-articular elbow flexors (STIMf). Co-contraction was defined as the amount of "shared" stimulation in STIMe and STIMf (Bullock and Contreras-Vidal 1993).

Table 1 Segment parameters

	length (m)	mass (kg)	I_Z (kgm^2)	Z [m]
Upper arm	0.335	2.10	0.024	0.146
Fore arm	0.263	1.65	0.025	0.179

I_Z = moment of inertia with respect to the centre of gravity Z = distance from proximal joint to centre of gravity
*Including hand

Table 2 Muscle parameters

Muscle	F_{MAX} (N)	l_{CE_opt} (m)	l_{SE_0} (m)	l_{PE_0} (m)	a_0 (m)	a_{1e} (m)	a_{1s} (m)	a_{2e} (m)
MEF	1420	0.092	0.172	0.129	0.286	−0.014	0	−3.96e-3
MEE	1550	0.093	0.187	0.130	0.236	0.025	0	−2.16e-3
BF	414	0.137	0.204	0.192	0.333	−0.016	−0.030	−5.73e-3
BE	603	0.127	0.217	0.178	0.299	0.030	0.030	−3.18e-3

The following parameters were equal for all muscles modelled: m = 11.30, c = 1.37 e-4, η = 5.27 e4, q_0 = 5.00 e-3, k = 2.90 and *width* = 0.66 For abbreviations see "List of symbols"

For any of the modelled muscles and for any combination of STIM, shoulder angle (φ_s) and elbow angle (φ_e), a value for l_{CE} can be calculated that results in an isometric situation, i.e. a situation in which the force of SE is equal to the sum of the forces of CE and PE (see Fig. 2 and Appendix). This was done for all muscles with STIM ranging from 0 to 1 in steps of 0.01, φ_e ranging from 0 to $\frac{5}{6}\pi$ rad in steps of 0.01 rad and φ_s ranging from 0 to $\frac{1}{2}\pi$ rad in steps of $\frac{1}{12}\pi$ rad. For any combination of φ_s and φ_e, all combinations of STIMe and STIMf were identified that yielded an open-loop EP, i.e. an EP achieved without the aid of feedback. For each EP found, the slope of the net isometric moment–angle relationship in the EP was estimated. To be consistent with the literature K_{ilf} was defined as minus the value of this slope. In other words, a positive value of K_{ilf} means that the EP is stable. Unstable EPs (i.e. EPs with negative K_{ilf}) were discarded.

3 Results

Figure 3a shows the maximal isometric moment–angle relationships of all modelled muscles at maximal stimulation in the range of elbow angles from 0 to $\frac{5}{6}\pi$ rad. The optimum angle for the moment–angle relationship of all flexors combined was set to be consistent with that found in measurements on human subjects (see Table 3). The same was done for the optimum angle of the moment–angle relationship of all extensors combined, but because this relationship is not well documented in the literature, estimation of the optimum angle may have been imprecise.

Table 3 Elbow angles at which the peak occurred in the isometric moment-angle relationship for elbow extension (φ_{opt_ext}) and elbow flexion (φ_{opt_flex})

Reference	φ_{opt_ext}	φ_{opt_flex}
An et al. (1989)	–	0.5π
Chang et al. (1999)	–	0.5π
Singh and Karpovitch (1968)	$\pm 0.5\pi$	0.5π
Van Zuylen et al. (1988)	–	0.56π[a]
Kullig et al. (1984)	$\pm 0.47\pi$	0.5π
This study	0.44π	0.53π

[a] Compensated for difference in angle definition

Figure 4 shows the stable EPs obtained, at three different shoulder angles. Stable EPs were found for all elbow angles in the physiological range of motion (0 to $\frac{5}{6}\pi$ rad), at all shoulder angles investigated (0 to $\frac{1}{2}\pi$ rad). For each STIM leading to a stable EP, it was confirmed by numerical simulations that regardless of the initial state of the system, the system moved towards the calculated EP and came to rest there. For all elbow angles considered, EPs could be realized with different combinations of STIMe and STIMf, and thus at different levels of co-contraction. In Fig. 4b, this is graphically shown as the intersection of the EP landscape with a horizontal plane: all the stimulation pairs on the intersecting curve lead to an EP at the same angle. As indicated in Fig. 4, results for different shoulder angles were qualitatively the same. For the sake of conciseness, in the remainder of this paper we shall present only results for the condition in which the shoulder angle was fixed at $\frac{1}{4}\pi$ rad.

In order to assess the contribution of LDCS to the static characteristics of the system, the model was also evaluated for stable EPs in the absence of LDCS (see

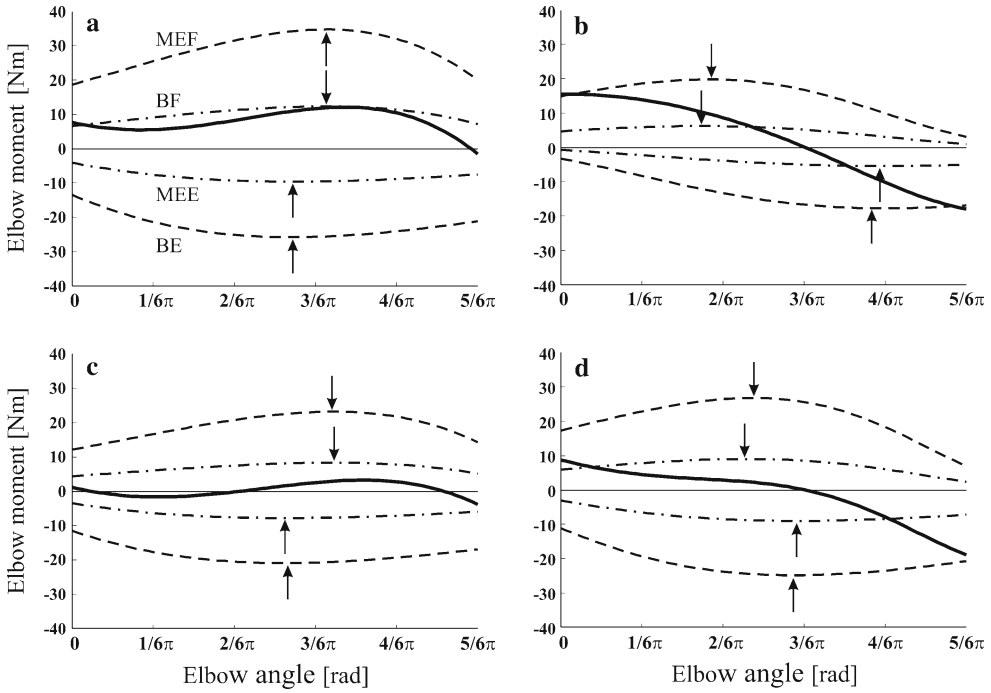

Fig. 3 Isometric moment–angle relations. (a) STIM = [1 1], (b) STIM = [0.17 0.22], (c) STIM = [0.17 0.22] without LDCS, (d) STIM = [0.25 0.55]. *Dashed* and *dash-dotted* lines are the isometric moment–angle relations of the individual muscles. *Arrows* indicate optimum angle for each muscle separately. *Solid line* is the resultant net moment

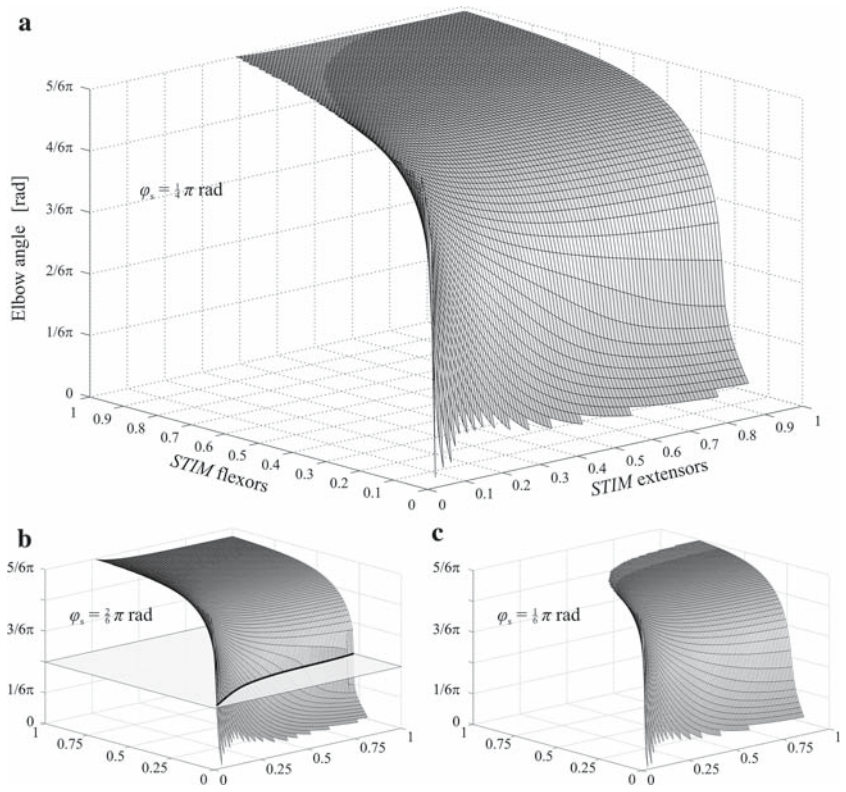

Fig. 4 Stable open-loop EPs as a function of muscle stimulation (STIM). STIMs leading to an EP at an elbow angle (φ_e) outside the range $0 - -\frac{5}{6}\pi$ rad were omitted. **a, b** and **c** show EPs at a shoulder angle (φ_s) of $\frac{1}{4}\pi$ rad, $\frac{2}{6}\pi$ rad and $\frac{1}{6}\pi$ rad, respectively. As illustrated in **b**, the intersection of the EP landscape with the horizontal STIM-plane represents all the combinations of STIM of the extensors and STIM of the flexors that yield an EP at the same elbow angle

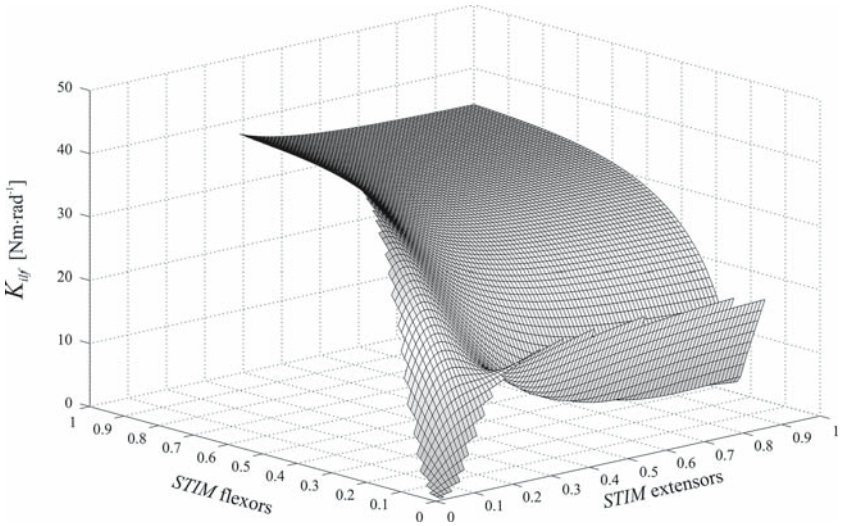

Fig. 5 Low-frequency stiffness (K_{ilf}) of the elbow joint as a function of STIM for all calculated stable EPs; in this particular case the shoulder angle was fixed at $\frac{1}{4}\pi$ rad (see Fig. 4a)

Appendix) and it was found that for many elbow angles, especially in the range between 0 and 2.3 rad, no EP could be obtained. Figure 3b, c illustrates the effect of the removal of LDCS. For a fixed STIM ([0.17 0.22]) leading to a stable EP at an angle of $\frac{1}{2}\pi$ rad, isometric moments as a function of elbow angle were calculated and plotted in Fig. 3b. A stable EP occurs at an angle where the net moment crosses zero with a negative slope (indicating stabilizing stiffness). In Fig. 3c, isometric moment–angle relationships were plotted with the same STIM ([0.17 0.22]), but without LDCS. Because lumping of the muscle stimulations might in principle reduce the range of angles over which stable EPs could be obtained, the model without LDCS was also evaluated for the existence of EPs when the muscle stimulations were not lumped, but controlled separately for each of the modelled muscles. In that case, the number of EPs increased, but none were found in the range of elbow angles between 0 and 1.8 rad.

From the model with LDCS, K_{ilf} was calculated for each STIM leading to an EP in the elbow angle range from 0 to $\frac{5}{6}\pi$ rad (for the condition in which the shoulder angle was fixed at $\frac{1}{4}\pi$ rad) (Fig. 5). The calculated K_{ilf} values were well within the (wide) range of values reported in literature for static conditions (Lacquaniti et al. 1982; Mussa-Ivaldi et al. 1985; MacKay et al. 1986; Flash 1987; Bennet et al. 1992). Higher K_{ilf} values were found when the combination of four individual muscle STIMs was optimized rather than the combination of two lumped STIMs. For example, at an elbow angle of $\frac{1}{2}\pi$ rad, maximal K_{ilf} was calculated to be about 19 N m·rad^{-1} when muscle stimulation was lumped and about 23 N m·rad^{-1} when the combination of individual muscle stimulations was optimized. To estimate the contribution of LDCS to K_{ilf}, elbow joint stiffness due to LDCS was calculated using Hatze's (1981) model of activation dynamics (see Appendix and Kistemaker et al. (2005)). The results indicated that this contribution was substantial; for some joint angles about 25 N m·rad^{-1} of the low-frequency CE stiffness could be attributed to LDCS.

Figure 6 shows the K_{ilf} for EPs ranging from 0 to $\frac{5}{6}\pi$ rad as a function of co-contraction level. Each line in the graph connects stimulations leading to an EP at one particular elbow angle (i.e. all the stimulations on the intersection curve of the EP landscape with a horizontal plane at a given elbow angle; see for example Fig. 4b). As can be seen in Fig. 6, K_{ilf} does not always increase when co-contraction is increased; K_{ilf} first increases with co-contraction to reach a peak value at a sub-maximal co-contraction level, and then drops when co-contraction is further increased. This non-monotonous relation between co-contraction and K_{ilf} is caused by LDCS. LDCS adds significantly to K_{ilf}, but the LDCS induced stiffness is absent for both high and low muscle stimulations, causing the total intrinsic stiffness to peak at a sub-maximal stimulation level (Kistemaker et al. 2005).

4 Discussion

The purpose of the present study was to investigate for the elbow joint whether the musculoskeletal system allows for setting stable EPs open-loop and to investigate the relationship between intrinsic low-frequency joint stiffness (K_{ilf}) and the level of co-contraction of elbow flexors and extensors. We attempted to extract from the literature the best estimate of each of the different variables influencing the static moment–angle–stimulation relationship of the muscles spanning the elbow joint.

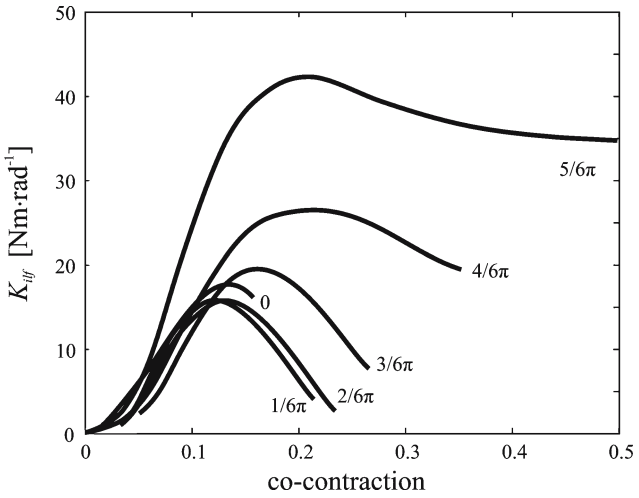

Fig. 6 Open-loop low-frequency stiffness (K_{ilf}) as a function of co-contraction level, which was defined as: min([$\mathrm{STIM}_e \mathrm{STIM}_f$]). Each line connects stimulations leading to a stable EP at the same angle (i.e. all the stimulations on the intersection of the EP landscape with a horizontal plane, see Fig. 4b)

In a previous study it was shown that Hatze's (1981) model of activation dynamics provides a good description of the effect of sarcomere length on the sensitivity of myofilaments to Ca^{2+} (LDCS) and the shift in optimum l_{CE} with (sub-maximal) muscle stimulation level (Kistemaker et al. 2005). In the present study, this model was combined with the optimum lengths of the muscles crossing the elbow joint, the maximal isometric forces, the moment arm–angle relationships and the angles at which the muscles are at optimum length as reported in the literature, to end up with isometric moment–angle relationships of the model that were similar to those reported by Singh and Karpovitch (1968); Kullig et al. (1984); Van Zuylen et al. (1988); An et al. (1989) and Chang et al. (1999).

For the so-called α-model (e.g. Hogan 1984; Bizzi and Abend 1983) stable open-loop EPs are the foundation for the control of posture and movement. When stable EPs can be set at any joint angle within the physiological range of motion, a movement to any desired position can be generated by changing the STIM combination from that corresponding to the current EP to that corresponding to the desired EP. Exploration with the musculoskeletal model used in this study suggested that at any angle in the physiological range of motion, stable EPs could be set. Furthermore, stable EPs could be realized at different levels of co-contraction and hence with different values for K_{ilf}. K_{ilf} obtained at different co-contraction levels depended on elbow angle (see Fig. 6); it ranged from about 18 N m·rad^{-1} near full extension to 43 N m·rad^{-1} at about $\frac{5}{6}\pi$ rad. It should be noted that the intrinsic low-frequency joint stiffness estimated in this study is lower than the total low-frequency joint stiffness for two reasons. Most importantly because no feedback was incorporated in the model, but also because lumping of muscle stimulation negatively affected the stiffness values predicted (see Results).

Indeed, the K_{ilf} values derived in this study were in the lower region of the wide range of total joint stiffness values (14–126 N m·rad^{-1}) reported in the literature (e.g. Bennet et al. 1992; Lacquaniti et al. 1993; Gomi and Osu 1998). The large variation of stiffness values supports the claim of Latash and Zatsiorsky (1993) that neither the definition nor the experimental determination of stiffness is without problems. In particular, Gomi et al.(Gomi and Kawato 1997; Gomi and Osu 1998) suggested that the large variation in reported stiffness values is related to differences in experimental set-up and instructions. As one example, in the study of Lacquaniti et al. (1982), in which stiffness values up to 126 N m·rad^{-1} were reported, subjects were instructed to maximally resist a deterministic perturbation. Because subjects knew beforehand that a perturbation was going to occur, it is quite likely that they modified the supra-spinal input to the muscles, which may explain why the "stiffness" reported was twice the maximal stiffness value reported in other studies (e.g. Gomi and Osu 1998; Popescu et al. 2003). As another example, stiffness is typically estimated by fitting a second-order model to the response to quasi-random perturbations. Latash and Zatsiorsky (1993) correctly argued that in this case the stiffness estimated depends on the frequency content of the perturbations. This is because in the intact musculoskeletal system, the skeleton interacts with a visco-elastic contractile element in series with an elastic tendon (and aponeurosis), resulting in a system that is at least of order three. As a consequence, the parameters of the KBI model fitted to the response to perturbations depend on the frequency content of the perturbation. This implies that, even though it has been shown that second-order models can approximate the response to small perturbations accurately (e.g. Agarwal and Gottlieb 1977; Hunter and Kearney 1982; Winters and Stark 1987), the stiffness identified using fast perturbations may well be higher than the low-frequency stiffness as defined in this study. All in all, the intrinsic low-frequency stiffness estimated in the present study makes a substantial contribution to the total stiffness as experimentally derived.

In the present study we found that a substantial part of K_{ilf} can be attributed to LDCS. Moreover, the contribution of LDCS to K_{ilf} turned out to be essential for the model to have stable open-loop EPs over the whole physiological range of motion; after LDCS had been

removed from the muscle model, there was a large part of the range of motion of the elbow for which no stable EPs could be obtained. The influence of LDCS for force generation can be best explained at the level of a single muscle. As mentioned briefly in the Introduction, LDCS causes an increase in Ca^{2+} sensitivity at higher CE length (Endo 1972, 1973; Stephenson and Williams 1982; McDonald et al. 1997; Patel et al. 1997; Konhillas et al. 2002), so that the CE length at which the largest isometric force is produced shifts to a value that is larger than l_{CE_opt} (e.g. Balnave and Allen 1996; Roszek et al. 1994). Thus, if a muscle is stretched to a new constant length, isometric muscle force not only changes as a result of changes in myofilamentary overlap but also changes (i.e. increases) as a result of LDCS. This means that, from a mechanical point of view, LDCS adds to the low-frequency stiffness of a muscle as defined in this study. It has been shown that LDCS peaks at sub-maximal stimulation levels (Endo 1972, 1973; Stephenson and Williams 1982; McDonald et al. 1997; Patel et al. 1997; Konhilas et al. 2002), which we have previously interpreted as an indication that LDCS-induced stiffness peaks at intermediate stimulation levels (Kistemaker et al. 2005). At the level of the joint, LDCS caused a shift in optimum joint angle for maximal isometric moment (see Fig. 3) and caused K_{ilf} to relate non-monotonically to co-contraction. For most elbow angles K_{ilf} peaked at a sub-maximal co-contraction level (see Fig. 6) of about 0.15. Note that, due to the highly non-linear relation between stimulation and active state in the activation dynamics model used (see Appendix), the isometric force of a muscle at a stimulation level of 0.15 is about 60% of maximal isometric force. It seems that LDCS allows us to realize a given level of stiffness at a lower force level and thus at lower metabolic cost. To exemplify the non-monotonic relationship between K_{ilf} and level of co-contraction, moment–angle relations were plotted for a co-contraction level that maximized K_{ilf} (Fig. 3b), as well as for a higher co-contraction level (Fig. 3d), both setting the EP at $\frac{1}{2}\pi$ rad. Although the level of co-contraction and the associated individual muscle moments were higher in Fig. 3d compared to Fig. 2b, K_{ilf} was smaller, as indicated by the less steep slope of the net moment–angle relationship in the EP.

The suggestion that K_{ilf} peaks at a sub-maximal level of co-contraction runs counter to the generally accepted notion that stiffness increases with co-contraction. Yet, this suggestion follows logically when LDCS, a well-documented physiological muscle property, is combined with the commonly used Hill-type muscle model. In our view, it would be interesting to test the suggestion experimentally. This would require an experiment and a method to tease apart the intrinsic and reflexive contributions to the total low-frequency joint stiffness. As to the experiment, it would seem straightforward to conduct an experiment in which stiffness and co-contraction level are not only measured when a subject is asked to maximally resist perturbations, but also when the subject is asked to maximally co-contract. If in the latter case both co-contraction and K_{ilf} are higher, it will falsify the suggestion made above. To our knowledge, such experiments have not been conducted so far. The relation between co-contraction and stiffness is typically measured during experiments in which a subject is asked to maintain a position while confronted with environmental instabilities (e.g. Osu and Gomi 1999; Milner 2002). In such a set-up, however, it is unlikely that subjects, when asked to resist these perturbations, will raise their co-contraction level beyond the level that maximizes stiffness. As to the teasing apart of intrinsic and reflexive contributions to the total low-frequency joint stiffness, one method that has been used is to subtract intrinsic stiffness estimated with a muscle model from the measured stiffness (Shadmehr and Arbib 1992). Obviously, such an approach would not be applicable to test our suggestion, because it is the intrinsic stiffness that needs to be estimated. Other methods reported in the literature build on system identification techniques (e.g. Kearney et al. 1997; Zhang and Rymer 1997; Van der Helm et al. 2002). In view of the intricacies of experimental determination of stiffness (Latash and Zatsiorsky 1993), it should be firmly established that the identification method to be used in the context of the envisaged experiment allows for unbiased estimation of the intrinsic low-frequency stiffness.

If the model-based prediction that stable open-loop EPs exist over the full physiological range of elbow joint motion is accepted, then a prerequisite for the α-model is satisfied; a controller based on the α-model would be capable of controlling movements from any initial position to any target position. However, the existence of stable open-loop EPs over the full range of motion is not sufficient for alpha-control to be feasible; it could well be, for example, that alpha-control is too sluggish. The dynamics of movements generated with different types of EP controllers, and their resemblance to fast movements produced by human subjects, are investigated elsewhere (Kistemaker et al. 2006).

Appendix

The modelled Hill-type muscle consists of CE, SE and PE, as shown schematically in Fig. 2 (see "List of symbols" for the relevant abbreviations).

STIM is related to active state (q; defined as the relative amount of Ca^{2+} bound to troponin;

Ebashi and Endo 1968), using Hatze's model of activation dynamics (1981). Steady state q is a non-linear function of STIM:

$$q = \frac{q_0 + (\rho \cdot \mathrm{STIM})^3}{1 + (\rho \cdot \mathrm{STIM})^3} \quad (1)$$

with q_0 a constant and ρ a function of $l_{\mathrm{CE\_rel}}$:

$$\rho = c\eta \frac{(k-1)}{(k - l_{\mathrm{CE\_rel}})} l_{\mathrm{CE\_rel}} \quad (2)$$

c, η and k are constants (see Table 2).

In order to assess the contribution of LDCS to the static characteristics of the system, the dependency of q on CE length was removed by fixing $l_{\mathrm{CE\_rel}}$ at a value of 1 in Eq. 2, making ρ independent of $l_{\mathrm{CE\_rel}}$, i.e. $\rho = c\eta$. This simplifies the dependence of q on STIM to:

$$q = \frac{q_0 + (c \cdot \eta \cdot \mathrm{STIM})^3}{1 + (c \cdot \eta \cdot \mathrm{STIM})^3} \quad (3)$$

Normalized isometric force ($F_{\mathrm{isom_n}}$) is modelled as a second-order polynomial with an optimum at $l_{\mathrm{CE\_rel}} = 1$ and two zero-crossings at $l_{\mathrm{CE\_rel}} = 1 \pm width$:

$$F_{\mathrm{isom\_n}} = -a \cdot {l_{\mathrm{CE\_rel}}}^2 + 2a \cdot l_{\mathrm{CE\_rel}} - a + 1 \quad (4)$$

with $a = 1/width^2$. This characteristic is scaled for q, F_{MAX} and $l_{\mathrm{CE\_opt}}$ (see Table 2) to end up with the isometric CE force (F_{isom}) as function of l_{CE}.

$$F_{\mathrm{isom}} = q \cdot F_{\mathrm{MAX}} \cdot F_{\mathrm{isom\_n}} \quad (5)$$

The parameter "*width*" was chosen such that the isometric moment–angle relationship of the model corresponded to measured relationships presented in literature. The passive force–length characteristic of the PE is modelled to depend quadratically on $l_{\mathrm{CE\_rel}}$ (note that $l_{\mathrm{PE}} = l_{\mathrm{CE}}$, see Fig. 2):

$$F_{\mathrm{PE}} = k_{\mathrm{PE}} \cdot \left[\max\left(0, l_{\mathrm{CE\_rel}} - \frac{l_{\mathrm{PE\_0}}}{l_{\mathrm{CE\_opt}}}\right)\right]^2 \quad (6)$$

k_{PE} is chosen such that $F_{\mathrm{PE}} = 0.5\ F_{\mathrm{MAX}}$ at $l_{\mathrm{CE\_rel}} = 1 + width$. The passive force characteristic of the *SE* is modelled to depend quadratically on l_{SE}:

$$F_{\mathrm{SE}} = k_{\mathrm{SE}} \cdot [\max(0, l_{\mathrm{SE}} - l_{\mathrm{SE\_0}})]^2 \quad (7)$$

k_{SE} is chosen such that SE is 4% elongated at F_{MAX}.

l_{MTC} as function of φ_{e} and φ_{s} is modelled as a second-order polynomial:

$$l_{\mathrm{MTC}}(\varphi_{\mathrm{e}}, \varphi_{\mathrm{s}}) = a_0 + a_{1\mathrm{e}} \cdot \varphi_{\mathrm{e}} + a_{2\mathrm{e}} \cdot {\varphi_{\mathrm{e}}}^2 + a_{1\mathrm{s}} \cdot \varphi_{\mathrm{s}} \quad (8)$$

$a_{1\mathrm{e}}, a_{2\mathrm{e}}$ and $a_{1\mathrm{s}}$ are based on cadaver data using tendon displacement method (Grieve et al. 1978). a_0, representing l_{MTC} at $\varphi_{\mathrm{e}} = \varphi_{\mathrm{s}} = 0$ (for angle definition see Fig. 1), is chosen such that optimum angles for maximal isometric moment is consistent with those reported in the literature. a_0 thus directly affects the angle at which CE length is optimal. Only insofar as moment arms are non-constant, it also indirectly affects the precise form of the torque–angle relation; this indirect effect is usually not substantial. Moment arms are calculated by taking the partial derivative of l_{MTC} with respect to φ_{e} and φ_{s}:

$$\mathrm{arm_e}(\varphi_{\mathrm{e}}) = \frac{\partial l_{\mathrm{MTC}}}{\partial \varphi_{\mathrm{e}}} = a_{1\mathrm{e}} + 2a_{2\mathrm{e}}\varphi_{\mathrm{e}} \quad (9)$$

$$\mathrm{arm_s}(\varphi_{\mathrm{s}}) = \frac{\partial l_{\mathrm{MTC}}}{\partial \varphi_{\mathrm{s}}} = a_{1\mathrm{s}} \quad (10)$$

References

Agarwal GC, Gottlieb GL (1977) Oscillation of the human ankle joint in response to applied sinusoidal torque on the foot. J Physiol 268(1):151–176

An KN, Kaufman KR, Chao EY (1989) Physiological considerations of muscle force through the elbow joint. J Biomech 22(11–12):1249–1256

Balnave CD, Allen DG (1996) The effect of muscle length on intracellular calcium and force in single fibres from mouse skeletal muscle. J Physiol 492 (Pt 3):705–713

Bennet DJ, Hollerbach JM, Xu Y, Hunter IW (1992) Time-varying stiffness of human elbow joint during cyclic voluntary movement. Exp Brain Res 88:433–442

Bizzi E, Abend W (1983) Posture control and trajectory formation in single- and multi-joint arm movements. Adv Neurol 39:31–45

Bullock D, Contreras-Vidal JL (1993) How spinal neural networks reduce discrepancies between motor intention and motor realization. In: Newell KM, Corcos DM (eds.), Variability and motor Control, Human Kinetics Publishers, Champaign pp 183–221

Chang Y, Su F, Wu H, An K (1999) Optimum length of muscle contraction. Clin Biomech 14:537–542

Ebashi S, Endo M (1968) Calcium ion and muscular contraction. Prog Biophys Mol Biol 18:125–138

Flash T (1987) The control of hand equilibrium trajectories in multi-joint arm movements Biol Cybern 57:257–274

Endo M (1972) Stretch-induced increase in activation of skinned muscle fibres by calcium. Nature New Biol 237:211–213

Endo M (1973) Length dependence of activation of skinned muscle fibres by calcium. Spring Harb Symp Quant Biol 37:505–510

Giszter SF, Mussa-Ivaldi FA, Bizzi E (1993) Convergent force fields organized in the frog's spinal chord. J Neurosci 13(2):467–491

Gomi H, Kawato M (1997) Human arm stiffness and equilibrium-point trajectory during multi-joint movement. Biol Cybern 76(3):163–171

Gomi H, Osu R (1998) Task-dependent viscoelasticity of human multijoint arm and its spatial characteristics for interaction with environments. J Neurosci 18(21):8965–8978

Graziano MSA, Taylor CSR, Moore T (2002) Complex movements evoked by microstimulation of precentral cortex. Neuron 34:841–851

Grieve DW, Pheasant S, Cavanagh PR (1978) Prediction of gastrocnemius length from knee and ankle joint posture. In: Asmussen E, Jorgensen K (eds.), Biomechanics VI-A, Inter-

national Series on Biomechanics, vol. 2A, University Park Press, Baltimore, pp 405–412
Hansen EA, Lee HD, Barrett K, Herzog W (2003) The shape of the force–elbow angle relationship for maximal voluntary contractions and sub-maximal electrically induced contractions in human elbow flexors. J Biomech 36(11): 1713–1718
Hatze H (1981) Myocybernetic control models of skeletal muscle. University of South Africa, Pretoria, pp 31–42
Hogan N (1984) An organizing principle for a class of voluntary movements. J Neurosci 4(11):2745–2754
Hunter IW, Kearney RE (1982) Dynamics of human ankle stiffness: variation with mean ankle torque. J Biomech 15(10): 747–752
Kearney RE, Stein RB, Parameswaran L (1997). Identification of intrinsic and reflex contributions to human ankle stiffness dynamics. IEEE Trans Biomed Eng 44(6):493–504
Kistemaker DA, Van Soest AK, Bobbert MF (2005) Length-dependent [Ca^2+] sensitivity adds stiffness to muscle. J Biomech 38(9):1816–1821
Kistemaker DA, Van Soest AJ, Bobbert MF (2006) Is equilibrium point control feasible for fast goal-directed single-joint movements? J Neurophysiol 95:2898–3012
Konhillas JP, Irving TC, Tombe PP (2002) Length-dependent activation in three striated muscle types of the rat. J Physiol 544(1):225–236
Kullig K, Andrews JG, Hay JG (1984) Human strength curves. Exerc Sport Sci Rev 12:417–466
Lacquaniti F, Licata F, Soechting JF (1982) The mechanical behavior of the human forearm in response to transient perturbations. Biol Cybern 44(1):35–46
Lacquaniti F, Carrozzo M, Borghese NA (1993) Time-varying mechanical behavior of multijointed arm in man. J Neurophysiol 69(5):1443–1464
Latash ML, Zatsiorsky VM (1993) Joint stiffness: myth or reality? Hum Mov Sci 12:653–692
MacKay WA, Crammond, DJ, Kwan, HC, Murphy JT (1986) Measurements of human forearm viscoelasticity. J Biomech 19(3):231–238
McDonald KS, Wolff MR, Moss RL (1997) Sarcomere length dependence of the rate of tension redevelopment and sub-maximal tension in rat and rabbit skinned skeletal muscle fibres. J Physiol 501(3):607–621
Milner TE (2002) Contribution of geometry and joint stiffness to mechanical stability of the human arm. Exp Brain Res 143:515–519
Murray WM, Delp SL, Buchanan TS (1995) Variation of muscle moment arms with elbow and forearm position. J Biomech 28(5):513–525
Murray WM, Buchanan TS, Delp SL (2000) The isometric functional capacity of muscles that cross the elbow. J Biomech 33(8):943–952
Mussa-Ivaldi FA, Hogan N, Bizzi E (1985) Neural, mechanical and geometric factors subserving arm posture in humans. J Neurosci 5:2732–2743
Nijhof E, Kouwenhoven E (2000) Simulation of multijoint arm movements In: Winters J, Grago P (eds.), Biomechanics and neural control of posture and movement Springer, Berlin Heidelberg New York, pp 363–372
Osu R, Gomi H (1999) Multijoint muscle regulation mechanisms examined by measured human arm stiffness and EMG signals. J Neurophysiol 81(4):1458–1468
Patel JR, McDonald KS, Wolff MR, Moss RL (1997) Ca^{2+} binding to troponine C in skinned skeletal muscle fibres assessed with caged Ca^{2+} and a Ca^{2+} fluorophore. J Biol Chem 28:6018–6027
Popescu F, Hidler JM, Rymer WZ (2003) Elbow impedance during goal-directed movements. Exp Brain Res 152(1):17–28
Roszek B, Baan GC, Huijing PA (1994) Decreasing stimulation frequency-dependent length-force characteristics of rat muscle. J Appl Physiol 77(5):2115–2124
Shadmehr R, Arbib MA (1992) A mathematical analysis of the force-stiffness characteristics of muscles in control of a single joint system. Biol Cybern 66(6):463–477
Singh M, Karpovitch VK (1968) Strength of forearm flexors and extensors in men and woman. J Physiol 25(2):177–180
Stephenson DG, Williams DA (1982) Effects of sarcomere length on the force–pCa relation in fast- and slow-twitch skinned muscle fibres from the rat. J Physiol 333:637–653
Tehovnik EJ (1995) The dorsomedial frontal cortex: eye and forelimb fields. Behav Brain Res 67(2):147–163
Van der Helm FC, Schouten AC, De Vlugt E, Brouwn GG (2002) Identification of intrinsic and reflexive components of human arm dynamics during postural control. J Neurosci Methods 119(1):1–14
Van Soest AJ, Bobbert MF (1993) The contribution of muscle properties in the control of explosive movements. Biol Cybern 69:195–204
Van Zuylen EJ, Van Velzen A, Denier van der Gon JJ (1988) A biomechanical model for flexion torques of human arm muscles as a function of elbow angle. J Biomech 21(3):183–190
Winter DA (1990) Biomechanics and motor control of human movement. second edn. Wiley, New York
Winters JM, Stark L (1987) Muscle models: what is gained and what is lost by varying model complexity. Biol Cybern 55(6):403–420
Zhang LQ, Rymer WZ (1997) Simultaneous and nonlinear identification of mechanical and reflex properties of human elbow joint muscles. IEEE Trans Biomed Eng 44(12):1192–11209
Zuurbier CJ, Lee-de Groot MB, Van der Laarse WJ, Huijing PA (1998) Effects of in vivo-like activation frequency on the length-dependent force generation of skeletal muscle fibre bundles. Eur J Appl Physiol Occup Physiol 77(6):503–510